

PROTOCLUSTERS IN THE Λ CDM UNIVERSE

TAMON SUWA,¹ ASAO HABE,² AND KOHJI YOSHIKAWA³

Received 2006 January 10; accepted 2006 June 12; published 2006 July 14

ABSTRACT

We compare the highly clustered populations of very high redshift galaxies with protoclusters identified numerically in a standard Λ CDM universe ($\Omega_0 = 0.3$, $\lambda_0 = 0.7$) simulation. We evolve 256^3 dark matter particles in a comoving box of side $150 h^{-1}$ Mpc. By the present day there are 63 cluster-sized objects of mass in excess of $10^{14} h^{-1} M_\odot$ in this box. We trace these clusters back to higher redshift, finding that their progenitors at $z = 4\text{--}5$ are extended regions of typically 20–40 Mpc (comoving) in size, with dark halos of mass in excess of $10^{12} h^{-1} M_\odot$ and are overdense by typically 1.3–13 times the cosmological mean density. Comparison with observations of Ly α -emitting galaxies at $z = 4.86$ and 4.1 indicates that the observed excess clustering is consistent with that expected for a protocluster region if Ly α emitters typically correspond to massive dark halos of more than $10^{12} h^{-1} M_\odot$. We give a brief discussion of the relation between the high-redshift concentration of massive dark halos and present-day rich clusters of galaxies.

Subject headings: cosmology: theory — galaxies: clusters: general — methods: numerical

1. INTRODUCTION

The formation and evolution of structure in the universe, such as galaxy clusters and large-scale structure, is one of the most important issues in astrophysics. Since clustering properties of galaxies in the distant universe provide important clues to this issue, many observations have been made in order to detect (proto)clusters of galaxies at high redshifts (Steidel et al. 1998, 2000; Campos et al. 1999; Pentericci et al. 2000; Rhoads et al. 2000; Ouchi et al. 2001, 2003; Miley et al. 2004). These deep surveys of galaxies, which have significantly advanced our understanding of the properties and distribution of galaxies at high redshifts, are equally important in constraining the underlying structure formation scenarios.

Venemans et al. (2002) showed a region around a radio galaxy in which the number density of Ly α emitters (LAEs) is much higher than the mean for the universe suggested by Rhoads et al. (2000) at $z = 4.1$. The region has size of 2.7×1.8 Mpc (physical) and mass of $\sim 10^{15} M_\odot$. More recently, Shimasaku et al. (2003) found that LAEs are clustered in an elongated region with a size of 20×50 Mpc (comoving) at $z = 4.86$, which is comparable to the size of present-day large-scale structures. In this elongated region, there is a 12 Mpc radius circular region with a high surface density of LAEs, which may be a progenitor of a galaxy cluster. They also estimated the bias parameter of the LAEs to be in the range of $b \sim 3\text{--}16$ for a spatially flat low-density cosmological model (Λ CDM model). The elongated distribution of the LAEs in this region has also been interpreted as part of large-scale structure, although observations by Shimasaku et al. (2004) of the same sky area but closer to us by 39 Mpc (comoving) does not show large structure. In addition, Hayashino et al. (2004) reported that the LAE distribution at $z = 3.1$ in their observed area shows broad large-scale structure. They claim that this structure is not easy to explain in the context of the standard CDM model. Ouchi et al. (2005) observed LAEs at $z = 5.7$ and discovered filamentary structures and voids.

Although these regions that have very high number densities

of LAEs are claimed to be protoclusters, there has not yet been enough detailed study of these possibilities. Therefore, we investigate the formation and evolution of galaxy clusters in the early universe using cosmological simulations. In this Letter we report some properties of simulated protoclusters at $z = 5$ and compare our numerical results with observations by Shimasaku et al. (2003) and Venemans et al. (2002).

2. METHOD

2.1. Numerical Method

We perform a cosmological N -body simulation with the particle-particle-particle-mesh (P^3M) algorithm (Hockney & Eastwood 1981). Our simulation code is the same as used in Yoshikawa et al. (2000), with parameters Hubble constant in units of $100 \text{ km s}^{-1} \text{ Mpc}^{-1}$, $h = 0.7$, density parameter $\Omega_0 = 0.3$, baryon density parameter $\Omega_b = 0.015 h^{-2}$, rms density fluctuation amplitude on a scale of $8 h^{-1}$ Mpc, $\sigma_8 = 1.0$, power-law index of the primordial density fluctuation $n = 1.0$, and cosmological constant parameter $\lambda_0 = 0.7$. We employ $N_{\text{DM}} = 256^3$ dark matter particles, each with a mass of $2.15 \times 10^{10} M_\odot$. The size of the comoving simulation box, L_{box} , is $150 h^{-1}$ Mpc, and the box is on the periodic boundary condition. This size of the box is large enough to realize a sufficient number of clusters and large-scale structures at $z = 0$. We use the spline (S2) softening function for gravitational softening, and the softening length, ϵ_{grav} , is set to $L_{\text{box}}/(10N_{\text{DM}}^{1/3})$ ($\sim 60 h^{-1}$ kpc in the comoving scale).

2.2. Identification of Dark Halos and Protoclusters

We identify dark halos in a manner similar to that of Suwa et al. (2003). First, we define densities of dark matter particles using an interpolation technique following the smoothed particle hydrodynamics method (Monaghan 1992), and pick up particles whose densities are more than the virial density. Next, we apply the hierarchical friends-of-friends (HFOF) method (Klypin et al. 1999) for the selected dense particles. The maximum linking length l_{max} in the HFOF method is defined as $0.2\bar{l}$, where \bar{l} is the mean interparticle distance for all (not only the dense) particles. Then we draw a sphere of which the center is on the densest particle of the group and seek the radius in which the mean density of total matter is equal to the virial density. We regard

¹ Center for Computational Sciences, University of Tsukuba, Tsukuba 305-8577, Japan; tamon@ccs.tsukuba.ac.jp.

² Division of Physics, Graduate School of Science, Hokkaido University, Sapporo 060-0810, Japan; habe@astro1.sci.hokudai.ac.jp.

³ Department of Physics, School of Science, The University of Tokyo, 7-3-1 Hongo, Bunkyo-ku, Tokyo 113-0033, Japan; kohji@utap.phys.s.u-tokyo.ac.jp.

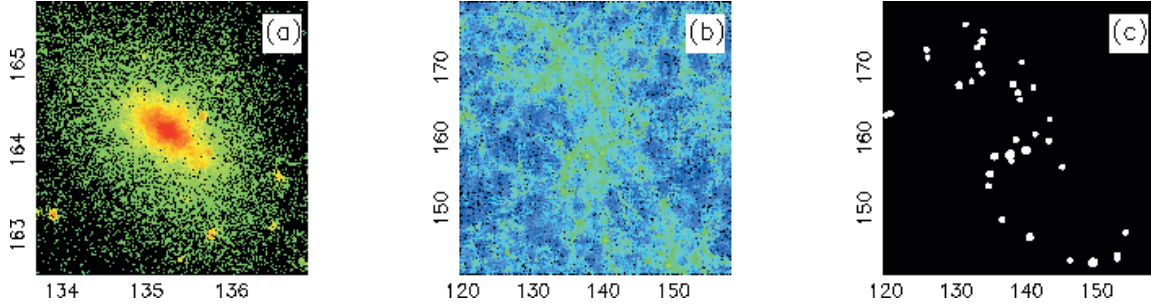


FIG. 1.—Distributions of dark matter and dark halos in an example cluster and the corresponding protocluster region in the simulation box. Panels *a* and *b* show the distribution of dark matter at $z = 0$ and $z = 5$, respectively. Panel *c* shows the distribution of dark halos that have mass $> 10^{12} h^{-1} M_{\odot}$ in the protocluster region shown in (*b*). The x - and y -axes are comoving position coordinate in the simulation.

the set of particles in the sphere as a virialized object. If a centroid of a sphere exists in another sphere, only the set that belongs to the more massive sphere is used. We regard dark halos that have mass of more than $10^{14} h^{-1} M_{\odot}$ at $z = 0$ as galaxy clusters, and we analyze properties of their progenitors to compare with the observations of protocluster regions (Venemans et al. 2002; Shimasaku et al. 2003).

We seek protoclusters in the high redshift universe as follows. First, we select all particles in each cluster at $z = 0$. Next, we trace those particles back to a high- z epoch, e.g., $z = 5$. Finally, we set a minimum cubic region that covers all of the particles. This region contains the protocluster of the present cluster, and we call it the “protocluster region” for the cluster.

In order to investigate galaxy distribution in the protocluster regions, we identify galaxy-size dark halos ($M > 10^{12} h^{-1} M_{\odot}$) in the regions at $z = 5$. Spatial distribution arguments (Hamana et al. 2004) suggest that dark halos of this mass scale are likely to contain LAEs and LBGs.

2.3. Overdensity

In protocluster regions, it is expected that dark halos that correspond to galaxies will concentrate much more densely than the background. Therefore, the excess number density of dark

halos, δ_{halo} , should be useful a quantity for comparing the results of the simulation to observations:

$$\delta_{\text{halo}} = (\bar{n}_{\text{halo}}/n_{\text{halo, BG}}) - 1, \quad (1)$$

where \bar{n}_{halo} is the halo number density averaged on a suitable scale (e.g., 25 Mpc) and $n_{\text{halo, BG}}$ is the background halo number density.

The mass overdensity, δ_{mass} , is defined in a similar way:

$$\delta_{\text{mass}} = (\rho/\rho_{\text{BG}}) - 1, \quad (2)$$

where ρ is the density of the region under consideration and ρ_{BG} is that of the background. The combination of the halo overdensity and the mass overdensity give us important information about mass concentration, so-called bias information, which has been investigated in analytical and numerical works (e.g., Kaiser 1984; Taruya & Suto 2000; Yoshikawa et al. 2001).

3. RESULTS

We find 63 galaxy clusters with $M > 10^{14} h^{-1} M_{\odot}$ in the simulation box at the present epoch ($z = 0$). We seek their progenitors, i.e., protoclusters, in the high-redshift universe and study their properties. Figure 1 shows an example of present-day galaxy clusters and protocluster regions in our simulation box at $z = 5$.

In our numerical results, the size of the protocluster regions is in the range of 20–40 Mpc in the comoving scale. This is similar to the size of the LAE-dense region observed by Shimasaku et al. (2003). Several dark halos with $M > 10^{12} h^{-1} M_{\odot}$ already exist in protocluster regions at $z = 5$, as shown in Figure 1c. We obtain the bulk velocity of each dark halo in the protocluster regions and find that their dispersion is typically $\sim 200 \text{ km s}^{-1}$.

We calculate δ_{halo} and δ_{mass} for each protocluster region at $z = 5$ by assuming a smoothing scale of 25 Mpc (comoving), which is a typical protocluster size in our numerical results. In order to show that the values of these indicators have significant excess over the mean value of the universe, we randomly select $(25 \text{ Mpc})^3$ regions in the simulation box and calculate δ_{halo} and δ_{mass} for these regions. The number of the randomly selected regions is 630, which is 10 times more numerous than the protocluster regions. We show the histograms of δ_{halo} in Figure 2, where the red solid line is for the protocluster regions and the green dashed line is for the randomly selected regions. The red solid line is significantly different from the green dashed line. Figure 2 shows that the typical value of δ_{halo} is ~ 3 for the

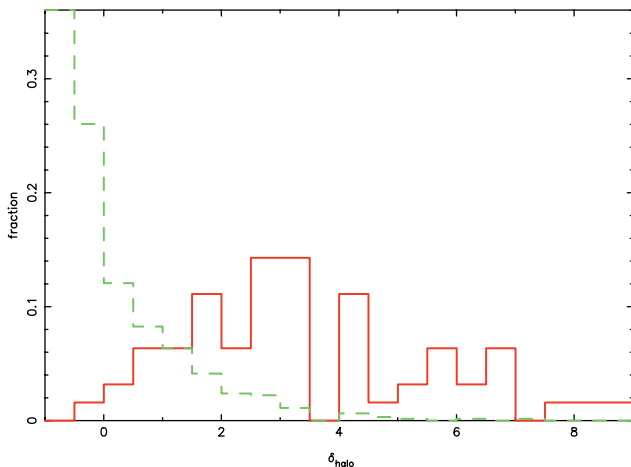
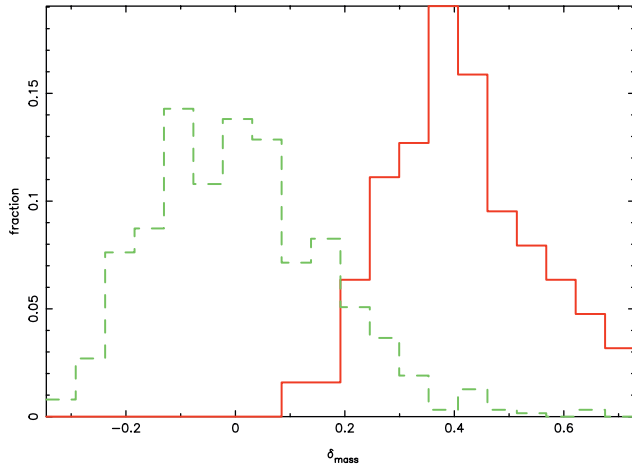


FIG. 2.—Histogram of halo number overdensities, δ_{halo} , of the protocluster regions (red solid line) and the randomly selected region (green dashed line) at $z = 5$.

FIG. 3.—Same as Fig. 2, but for δ_{mass} .

protocluster regions, and its variance is very large. On the other hand, δ_{halo} in most of the randomly selected regions is almost -1 ; this value means that there is no massive dark halo in the regions.

The mass overdensities, δ_{mass} , for the protocluster regions are clearly different from those for the randomly selected regions as shown in Figure 3. The δ_{mass} of the protocluster regions are in the range of 0.2–0.4, while those of the randomly selected regions range from -0.2 to 0.2. The typical value of δ_{mass} in the protocluster regions is ~ 0.4 , and the variance of δ_{mass} is much smaller than that of δ_{halo} .

In order to show the bias of the dark matter halo distribution in the protocluster regions, in Figure 4 we plot δ_{mass} and δ_{halo} for the protocluster regions and the randomly selected regions. Red triangles, blue crosses, and green squares indicate the protocluster regions, randomly selected regions that overlap more than 50% with some protocluster region, and other randomly selected regions, respectively. Figure 4 shows a correlation between the values of δ_{halo} and δ_{mass} for $\delta_{\text{mass}} > 0$, although the dispersion is very large. It is clear that the regions with large δ_{mass} have large δ_{halo} . This relation corresponds to the bias of the dark matter halo distribution in the protocluster regions.

We compare the $\delta_{\text{mass}}-\delta_{\text{halo}}$ relation in our numerical results with the analytical result given by the natural bias theory (Mo & White 1996) in Figure 4. In Figure 4, we show the analytical relation by a thick black line; we use the Press-Schechter mass function formula and the relation of linear extrapolation to nonlinear evolution for density perturbations (Carroll et al. 1992). Green and red lines in Figure 4 indicate the average values of the randomly selected regions and the protoclusters, respectively. The $\delta_{\text{mass}}-\delta_{\text{halo}}$ relation given by the natural bias theory agrees well with our numerical results, as shown in Figure 4, except for a gradual deviation at $\delta_{\text{mass}} > 0.4$. This deviation can be explained by the limiting effect of our simulation box size, which is not large enough to consider large-scale ($100 h^{-1}$ Mpc) components of density fluctuation; this limitation may cause an underestimation of the mass function for $10^{12} M_{\odot}$ dark halos at $z = 5$ (Bagla & Ray 2005).

It is very important to find a critical value of δ_{halo} , $\delta_{\text{halo},c}$, by which we can select a protocluster region. In order to identify $\delta_{\text{halo},c}$, we compare values of halo overdensity, δ_{halo} , in the randomly selected regions at $z = 5$ and masses of the largest dark halos in the regions at the present epoch. Figure 5 shows

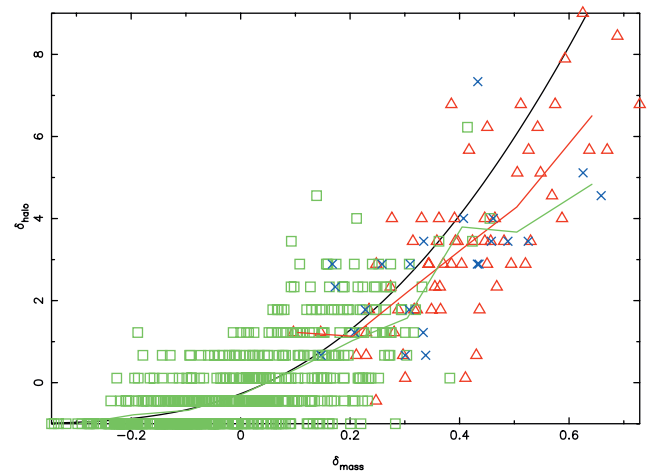


FIG. 4.—Correlation map of δ_{mass} and δ_{halo} . Red triangles, blue crosses, and green squares indicate the protocluster regions, randomly selected regions that overlap more than 50% with some protocluster region, and other randomly selected regions, respectively. The analytical relation is indicated by a thick black line. Green and red lines correspond to average value of simulated regions randomly selected (both field and overlap) and protoclusters, respectively.

the fraction of the regions that contain galaxy clusters with $M > 10^{14} h^{-1} M_{\odot}$ at $z = 0$ as a function of δ_{halo} at $z = 5$. It is clear from this figure that most regions with $\delta_{\text{halo}} \geq 3$ at $z = 5$ will evolve rich clusters with mass of more than $10^{14} h^{-1} M_{\odot}$ at $z = 0$.

4. DISCUSSION

We have investigated protocluster regions and the difference between these and background field regions using an N -body cosmological code. In order to investigate protoclusters, we identify 63 galaxy clusters in our cosmological simulation at $z = 0$, and trace dark matter particles that belong to these back to a high-redshift epoch. We study the properties of the protocluster regions by analyzing the mass overdensity, δ_{mass} , and the halo overdensity, δ_{halo} (see § 2). The results at $z = 5$ are shown in Figures 2, 3, and 4. As expected from bias theory

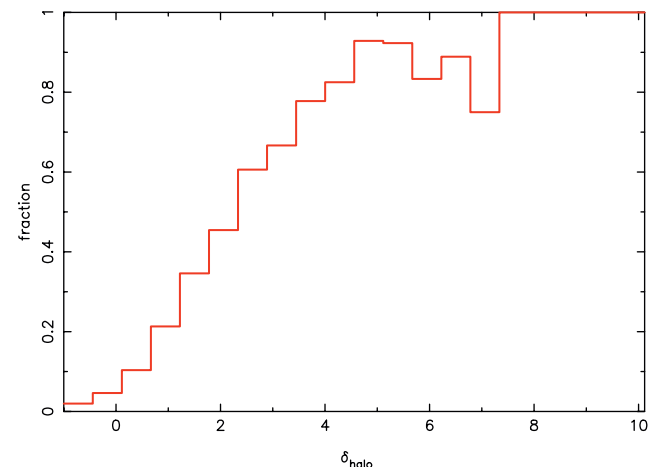


FIG. 5.—Fraction of randomly selected cubic regions that contain a galaxy cluster at $z = 0$ as a functions of δ_{halo} at $z = 5$. The size of the cubic regions is 25 Mpc (comoving).

(e.g., Taruya & Suto 2000), δ_{halo} shows excess over δ_{mass} , and the variance of δ_{halo} is much larger than that of δ_{mass} .

In order to show the difference between the protocluster regions and the field, we calculate δ_{mass} and δ_{halo} for randomly selected regions with the same size as the typical protocluster region at $z = 5$ (25 Mpc in the comoving scale). We select 630 randomly selected regions (10 times the number of protocluster regions). Clustering properties of the dark halos in these regions are significantly different from those in the protocluster regions. The halo overdensities for most of the randomly selected regions are much smaller than those for the protocluster regions, as shown in Figure 2.

We are also interested to find critical value of δ_{halo} by which we can select a protocluster region. From Figure 5, we have found that more than 80% of the regions with $\delta_{\text{halo}} \geq 3$ at $z = 5$ contain rich clusters ($M \geq 10^{14} h^{-1} M_{\odot}$) at the present epoch. Thus, we conclude that $\delta_{\text{halo}} \geq 3$ is a good criterion to distinguish protocluster from field regions at $z = 5$. This criterion should be very useful to judge whether observed galaxies excess regions are actual protoclusters or not.

It should be pointed out that there are a few regions that do not contain clusters at $z = 0$ but that have large δ_{halo} values (3–7) at $z = 5$, although the fraction of those regions is very small. We suggest that the physical origin of the large δ_{halo} in these cases is nonlinearity and stochasticity of bias parameters, as proposed by Taruya & Suto (2000). They studied the variance of biasing parameters, and concluded that the variance increases strongly with redshift. They also concluded that the stochasticity of the biasing is generated by the scatter in the halo mass distribution at higher redshift. Yoshikawa et al. (2001) confirmed these results for $0 < z < 3$ by a large P^3M simulation. We conclude that our results for $z = 3$ are consistent with their results, and that the trend of the evolution of bias variance is still true for $3 < z < 5$.

We compare our results with the observation of Shimasaku et al. (2003). They report the following properties of the LAE-

concentrated region. (1) The diameter of the region is 25 Mpc (comoving unit). (2) The projected overdensity of LAEs $\delta_{\text{v}} \sim 2$. (3) The bias parameter is estimated to be 3–16 for Λ CDM model, and the best-fit value is $b \sim 6$, i.e., $\delta_{\text{mass}} \sim 0.3$. (4) The number of LAEs in the region is about 20. Properties 1–3 are consistent with our numerical results for protocluster regions, if LAEs correspond to dark halos more massive than $10^{12} h^{-1} M_{\odot}$, as suggested by Hamana et al. (2004) using the correlation function on small scales. The typical number of dark halos in the simulated protoclusters is 5–10, which is about half the number of observed LAEs. One explanation for this discrepancy is the possibility that some dark halos have more than one LAE. We speculate that some pairs of LAEs in Figure 3 of Shimasaku et al. (2003) are included in the same dark halo. It is also possible that some of the observed sample of LAEs in the region are low-redshift interlopers. Shimasaku et al. (2003) estimate the contamination of their sample to be about 20%.

Venemans et al. (2002) also reported properties of an LAE-rich region. The size of the region is $\sim 14 \times 10$ Mpc (comoving). They estimate that the region is overdense in LAEs by a factor of 15 compared with the blank field (Rhoads et al. 2000). The overdensity is much larger than that of protoclusters at $z = 4$ in our simulation, and the size of their observed region is smaller than the typical size of the protoclusters in our simulation. Therefore, we suggest that the region observed by them is not a whole protocluster region, but the central region of the protocluster, because of small size of the observed region and the high overdensity value.

We would like to thank Masayuki Fujimoto and Takayuki Saitoh for helpful advice, insightful discussions, and encouragement. We are also grateful to Tom Broadhurst for useful comments. Numerical computations used in this work were carried out on SGI Onyx300 at the Hokkaido University Computing Center by parallel computation with 16 CPUs.

REFERENCES

- Bagla, J. S., & Ray, S. 2005, MNRAS, 358, 1076
 Campos, A., Yahil, A., Windhorst, R. A., Richards, E. A., Pascarelle, S., Impey, C., & Petry, C. 1999, ApJ, 511, L1
 Carroll, S. M., Press, W. H., & Turner, E. L. 1992, ARA&A, 30, 499
 Hamana, T., Ouchi, M., Shimasaku, K., Kayo, I., & Suto, Y. 2004, MNRAS, 347, 813
 Hayashino, T., et al. 2004, AJ, 128, 2073
 Hockney, R. W., & Eastwood, J. W. 1981, Computer Simulation Using Particles (New York: McGraw-Hill)
 Kaiser, N. 1984, ApJ, 284, L9
 Klypin, A., Gottlöber, S., Kravtsov, A. V., & Khokhlov, A. M. 1999, ApJ, 516, 530
 Miley, G. K., et al. 2004, Nature, 427, 47
 Mo, H. J., & White, S. D. M. 1996, MNRAS, 282, 347
 Monaghan, J. J. 1992, ARA&A, 30, 543
 Ouchi, M., et al. 2001, ApJ, 558, L83
 Ouchi, M., et al. 2003, ApJ, 582, 60
 ———. 2005, ApJ, 620, L1
 Pentericci, L., et al. 2000, A&A, 361, L25
 Rhoads, J. E., Malhotra, S., Dey, A., Stern, D., Spinrad, H., & Jannuzi, B. T. 2000, ApJ, 545, L85
 Shimasaku, K., et al. 2003, ApJ, 586, L111
 ———. 2004, ApJ, 605, L93
 Steidel, C. C., Adelberger, K. L., Dickinson, M., Giavalisco, M., Pettini, M., & Kellogg, M. 1998, ApJ, 492, 428
 Steidel, C. C., Adelberger, K. L., Shapley, A. E., Pettini, M., Dickinson, M., & Giavalisco, M. 2000, ApJ, 532, 170
 Suwa, T., Habe, A., Yoshikawa, K., & Okamoto, T. 2003, ApJ, 588, 7
 Taruya, A., & Suto, Y. 2000, ApJ, 542, 559
 Venemans, B. P., et al. 2002, ApJ, 569, L11
 Yoshikawa, K., Jing, Y. P., & Suto, Y. 2000, ApJ, 535, 593
 Yoshikawa, K., Taruya, A., Jing, Y. P., & Suto, Y. 2001, ApJ, 558, 520